Hindawi
Shock and Vibration
Volume 2021, Article ID 8086094, 17 pages
https://doi.org/10.1155/2021/8086094

Research Article

Experimental Study on Mechanical Damage and Fracture Characteristics of Granite under Different Water Cooling Conditions

Zhuangzhuang Yao [1,2] Zhigang Zhang [1,2] Wenbin Wu [1,2] and Jiang Wu [3]

[1] *State Key Laboratory of the Gas Disaster Detecting, Preventing and Emergency Controlling, Chongqing 400037, China*
[2] *China Coal Technology and Engineering Group Chongqing Research Institute, Chongqing 400037, China*
[3] *Jinan Urban Construction Group Co., Ltd., Jinan 250031, China*

Correspondence should be addressed to Zhuangzhuang Yao; 759503455@qq.com

Received 12 August 2021; Revised 17 October 2021; Accepted 28 October 2021; Published 19 November 2021

Academic Editor: Bangbiao Wu

In order to investigate the mechanical property deterioration and fracture characteristics of granite under different temperature drop and thermal cycle conditions, the evolution laws of mechanical properties, acoustic emission event distribution, and macro and micro failure characteristics of granite under different temperature changes were studied and analyzed by the servo loading, acoustic emission monitoring, and scanning electron microscope systems. The following conclusions were gained from the test results. (1) The peak stress and elasticity modulus of the three temperature drop treatments all decreased with the increase of the number of thermal cycles. In terms of magnitude, the following relationship was satisfied: 10°C > 15°C > 20°C. After 8 cycles, the peak stress and elasticity modulus tended to be stable for 15°C and 20°C temperature drops. (2) At a temperature drop of 20°C, the heterogeneity first increased and then tended to be stable; when the temperature was dropped by 15°C at each cycle, however, the heterogeneity first decreased and then became stable; as for the case of 10°C, the heterogeneity showed an overall decreasing trend. After 4 cycles, the heterogeneities were ranked as 15°C > 20°C > 10°C. After 8 cycles, 20°C > 15°C > 10°C. (3) With the decrease of temperature drop amplitude or the increase of cycles, the connectivity of microcracks in granite improved on the whole, the aperture and shape factor of microcracks increased, the damage of granite intensified, and the duration of the quiet period in the acoustic emission ringing count rate prolonged. (4) The tensile failure dominated at a temperature drop amplitude of 10°C. When the temperature drop was 15°C, the failure mode transitioned from hybrid tension-shear failure to tensile failure as the cycle times increased, whereas the hybrid tension-shear failure dominated with a temperature drop of 20°C.

1. Introduction

With the deepening of underground rock mass projects, high-temperature issues become more common, including enhanced geothermal exploitation, nuclear waste storage, coal mining, and carbon dioxide storage, which have constituted as a major factor restricting the development of deep rock mass engineering [1]. Due to the interference of external factors such as the refrigerant medium, the temperature of the rock mass can change repeatedly, such as hydraulic fracturing in enhanced geothermal exploitation, which may lead to the deterioration of its mechanical properties, or even its instability in serious cases, causing heavy economic losses. Therefore, it is of great significance to study the mechanical behavior and failure characteristics of rocks under thermal cycles for the construction of deep rock mass projects.

Plenty of studies have been carried out in China and beyond regarding the influence of high-temperature thermal cycles on mechanical properties and failure characteristics of rocks. Yu *et al.* [2] investigated the evolution of mechanical properties for granite under high-temperature cycles and found that with the increase of cycle times, the compressive strength of granite weakened, whereas the sample failure mode changed from splitting tensile failure to conical shear failure. Xie *et al.* [3] believed that with the increase of the number of cycles, the uniaxial compressive strength of granite decreased, the shaping characteristics became more significant, while the acoustic emission signal characteristics showed a decreasing trend. With laboratory tests, Rong *et al.* [4] found that the mechanical damage of granite was limited by the number of cycles under a high temperature of 300°C. When the number of cycles exceeded 12, the tensile and compressive strengths of granite remained stable, no longer demonstrating aggravated damage. Through the Brazilian splitting test, Li *et al.* [1] proved that the tensile strength of granite decreased with the increase of the number of thermal cycles, though the attenuation in tensile strength was primarily controlled by the temperature. Peng *et al.* [5] investigated the variation law of micro thermal cracks in fine granular marble treated at 600°C as a function of the cycle times. The results showed that the microcracks in the marble were primarily intergranular cracks, the length and width of which increased with the number of cycles. Gautam *et al.* [6] analyzed the variations in damage of different granites at 250°C when the cycle times were varied. The results showed that the tensile strength and elasticity modulus of different types of granites both decreased with the increase of the number of cycles. When the number of cycles exceeded 5, however, further increase in cycle times had little impact on the damage of granite. Pathiranagei and Gratchev [7] analyzed the relationship between porosity, uniaxial compressive strength, and elasticity modulus of sandstone and the temperature conditions and cycle times, finding that when the temperature exceeded 600°C, with the increase of cycles, the porosity of sandstone significantly increased, whereas its uniaxial compressive strength and elasticity modulus decreased remarkably. Yu *et al.* [8] obtained the variation rule of compressive modulus and elasticity modulus of granite when treated with 300°C cycles, both demonstrating a decreasing trend with the increase in cycle times. Zhao *et al.* [9] believed that the temperature was a main factor affecting the pore structure of granite, while the influence of the number of high-temperature cycles was negligible.

In summary, great achievements have been made in the study on the influence of high temperature on mechanical properties of rocks. However, most of these studies set the target temperature of each cycle as a constant. In fact, in the construction of deep rock engineering, the temperature of reservoir rock usually changes in varying degrees due to the interference of external factors, for example, in the process of hydraulic fracturing of enhanced geothermal reservoir, due to the continuous injection of cold water from the outside, the temperature of the injected wellbore decreases faster than its temperature recharge, which makes the injected wellbore subjected to the phenomenon of variable high-temperature cycle. Different from the constant high-temperature cycle treatment, the damage of the reservoir rock mass under the variable high temperature condition will weaken with the increase of cycle times. As a result, if the research results from the constant temperature are used to guide the operating condition in variable temperature cycles, the evaluation result can be unduly serious with a higher maintenance level and cost as the detail and rule of rock damage weakening are ignored. There is little research on the problem of variable high-temperature cycle. Therefore, it is necessary to further study the deterioration of mechanical properties and fracture characteristics for rocks under variable high-temperature thermal cycles.

In the present study, granite was taken as the research object, and rock compression tests were carried out under variable high-temperature cycles with a temperature drop of 10°C, 15°C, and 20°C, respectively. By comparing and analyzing the physical and mechanical parameters of rocks, such as the compressive strength, acoustic emission characteristics, and macro and micro failure forms, the evolution rules of mechanical properties and failure characteristics of granite treated by various temperature-varying thermal cycles were obtained. The test results could provide theoretical guidance for deep project construction.

2. Sample Preparation and Test Scheme Design

2.1. Sample Preparation. The granite samples used in the test were taken from Laizhou, Shandong Province, with an average density of $2.69\,g/cm^3$. The samples were relatively compact in structure with no apparent macroscopic cracks. In order to reduce the influence of other factors, all the test samples were drilled from the same direction of one specimen. According to the recommended methods from the international rock mechanics test procedures [10], the granite was processed into a large number of cylindrical $\varphi 35 \times 70$ samples with a diameter-to-height ratio of 1 : 2, the end face error of which should not exceed 0.2 mm.

2.2. Test Scheme Design

2.2.1. Heating Scheme Design. In the heating test, due to the temperature of the global enhanced geothermal system is mostly between 200°C and 400°C, so 300°C is chosen as the highest target temperature in this paper. 10°C, 15°C, and 20°C temperature drop amplitudes were selected as the temperature variables. For each amplitude, 4, 8, and 12 thermal cycles were carried out, respectively. There were 9 groups of tests, each group of which was repeated for 3 times, yielding 27 samples in total. The heating test was conducted in a muffle furnace. The heating scheme is shown in Figure 1, and the specific heating procedures are as follows.

(1) Taking the 10°C temperature drop case as an example, 9 room temperature samples were first put into the muffle furnace and heated to the target temperature of 300°C at a rate of 5°C/min [11–16]. In order to ensure even heating of the whole sample, the target temperature was maintained for 8 h. Then the heated granite was quickly put into static water at room temperature (25°C) until the sample was cooled to room temperature (25°C) as well, it is the first cycle.

(2) The granite sample cooled to room temperature was then put into the muffle furnace again and heated to

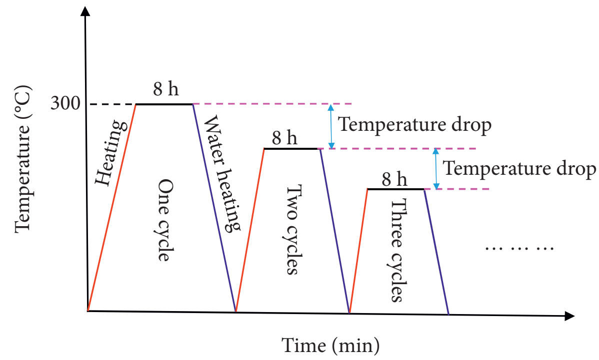

Figure 1: Schematic diagram of the sample heating-cooling scheme.

the target temperature of 290°C with the same heating rate. Keep the temperature for 8 h and then quickly put the heated granite into room temperature water until it was cooled to room temperature (25°C) again, it is the second cycle.

(3) Repeat step (2), heating samples to the target temperature of 280°C at the same rate and then cooling to the room temperature is the third cycle, and so on for the fourth cycle, the fifth cycle, and the 12th cycle. Three of the samples were taken out after 4 thermal cycles, three other samples were taken out after 8 cycles, and the remaining three samples were taken out after 12 cycles.

Then, follow the steps of (1), (2), and (3) to complete the tests when the temperature drop amplitudes was set to be 15°C or 20°C instead. The samples treated by the thermal cycles are shown in Figure 2.

2.2.2. Scheme Design of the Loading Test. The uniaxial compression test designed in this study was completed on a Shimadzu AG-X250 electronic universal testing machine. The displacement control mode was adopted in the loading process, and the loading rate was 0.01 mm/s until the specimen was damaged. During the loading process, the PCI-2 acoustic emission system was used to synchronously monitor the acoustic emission signal, the system threshold value is set to 40 dB, and the floating threshold is ik6 dB. Also, the whole process from crack propagation to failure and instability in the granite was recorded, as shown in Figure 3.

3. Test Results and Analyses

3.1. Variation of Apparent Characteristics in Granite Treated by Uniform Temperature Drops and Thermal Cycles. It can be seen from Figure 4 that the apparent characteristics of granite changed significantly after treatments with different temperature drops and thermal cycles. In all temperature drop cases, the surface color of granite altered from local light yellow to overall white with the increase of cycle times. Black spots obviously appeared on the sample surfaces, indicating that the high temperature led to the oxidation of biotite, the main component of the mineral. It should be noted that the changes in apparent characteristics were particularly evident when the temperature drop gradient was 10°C as in this scenario several macro cracks with unequal lengths appeared on the granite surface after 8 or 12 cycles.

3.2. Influence of Uniform-Amplitude Temperature Drops and Thermal Cycles on Mechanical Properties of Granite

3.2.1. Influence of Uniform-Amplitude Temperature Drops and Thermal Cycles on Peak Stress of Granite. Figure 5 shows the variation rule of peak stress of granite with the temperature drop amplitude. The arithmetic mean value of the three test data in each group was used to evaluate the influence of the temperature drop amplitude and thermal cycle on the deterioration of mechanical properties of granite. It can be seen from the figure that when the number of cycles was fixed, the average peak stresses in the three temperature drop cases satisfied the following relationship: 20°C > 15°C > 10°C. With the increase of thermal cycles, the repeated action of thermal stress promotes the development of cracks in granite, and the peak stress values further decreased in all three conditions. Besides, a smaller temperature drop amplitude corresponded to more serious damage in granite structure and a larger reduction in peak stress due to the cumulatively superimposed thermal stress. After 8 cycles, the peak stress tended to be stable for the cases with a temperature drop gradient of 15°C or 20°C, which indicated that the target heating temperature in these two conditions was lower than the threshold temperature of microcracks initiation and microcracks development. Therefore, the thermal stress generated by heating and cold shocks was lower than the secondary microcrack activation condition, allowing the effect of thermal cycles on the mechanical properties of granite to be ignored in these two cases.

3.2.2. Influences of Uniform-Amplitude Temperature Drops and Thermal Cycles on Elasticity Modulus and Crack Initiation Stress Level of Granite. Elasticity modulus is an important index to evaluate the mechanical properties of rock [17–20], which can reflect the deterioration of mechanical properties due to external factors. Therefore, this part explores the variation law of the elasticity modulus of granite with temperature drop gradients and the number of cycles.

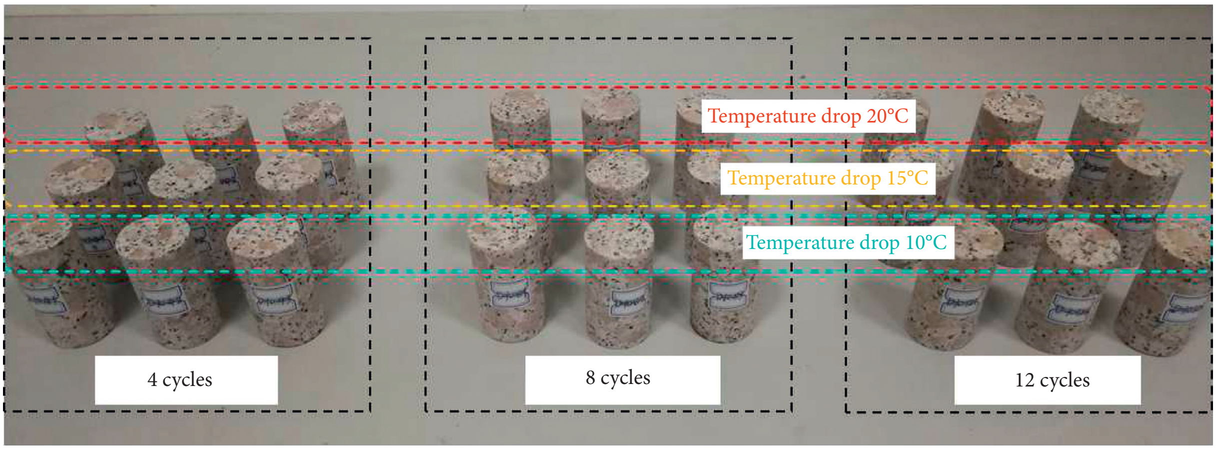

Figure 2: Granite samples treated with different temperature drop gradients.

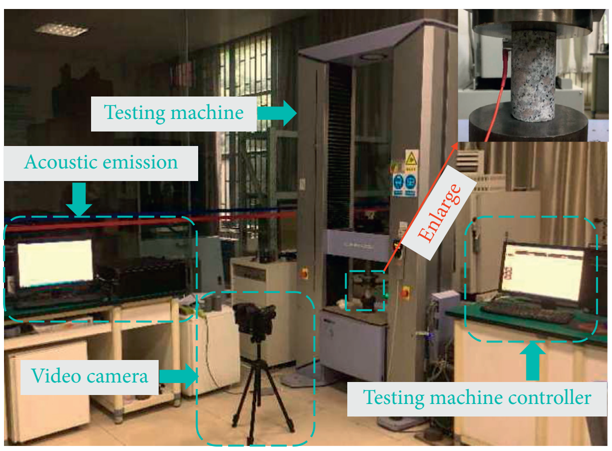

Figure 3: Photo of the testing equipment.

As can be seen from Figure 6(a), after treatments with different temperature drop amplitudes, the elasticity modulus decreased with the number of cycles, but tended to be stable after 8 cycles when the temperature drop was 15°C or 20°C. With the same number of cycles, the elasticity modulus demonstrated a certain regularity: 20°C temperature drop case >15°C temperature drop case >10°C temperature drop case.

The crack initiation stress level is generally defined as the ratio of the crack initiation stress to the peak stress of the rock:

$$k = \frac{\sigma_{ci}}{\sigma_c}, \quad (1)$$

where k is the crack initiation stress level of the rock; σ_{ci} is the crack initiation stress, MPa; and σ_c is the peak stress, MPa.

We can determine the initiation stress by acoustic emission ringing count rate. At the initial stage of loading, the original crack in granite is compacted and closed, and the acoustic emission ringing count rate can hardly be detected at this stage. With the increase of axial load, the AE signal begins to increase and become dense, and the granite reached the stress threshold of crack initiation. The location of crack initiation stress is marked in Figure 7.

Rock is a heterogeneous material, which contains a large number of micro-cracks and other defects. When subjected to external loads, local stress concentration occurs at the tip of microcracks, leading to crack initiation and propagation. Therefore, the crack initiation stress level of rock can reflect the heterogeneity and structural difference of rock. The smaller the value is, the stronger the heterogeneity of rock is [21–24]. The granite showed different degrees of heterogeneity after different temperature drops and cycle times.

As can be seen from Figure 6(b), the crack initiation stress level of granite was between 0.2 and 0.4 after treatments with different temperature drops and cycles. At a temperature drop amplitude of 20°C, the crack initiation stress level of granite first decreased then became stable with the increase in cycle times. This indicated that with the increase of the number of cycles, the cumulative heating stress promoted the random development of microcracks in different directions, increased the density of microcracks, and reduced the heterogeneity of granite. However, after 8 cycles, the target heating temperature became lower than the threshold temperature to initiate microcracks, the microcracks started to enter a dormant state, and the crack initiation stress level tended to be stable. For a temperature drop of 15°C, the crack initiation stress level of granite increased first and then became stable with the increase in the number of cycles. This showed that with the increase of cycle times, the microcracks connected with each other, forming weak plane structures with a larger size. The total number of microcracks then decreased, which resulted in an improvement of the heterogeneity instead. When the temperature was reduced by 10°C at each cycle, the weak plane structures of granite became more common, and the decrease of the crack initiation stress level became more evident with the increase of cycle times. This phenomenon could also be explained by Figure 5(a), in which after 8 cycles, several macroscopic thermal cracks appeared on the granite surface. After 12 cycles, the crack length was significantly increased compared with the case of 8 cycles.

When the number of thermal cycles was four, the crack initiation stress level of granite decreased first and then

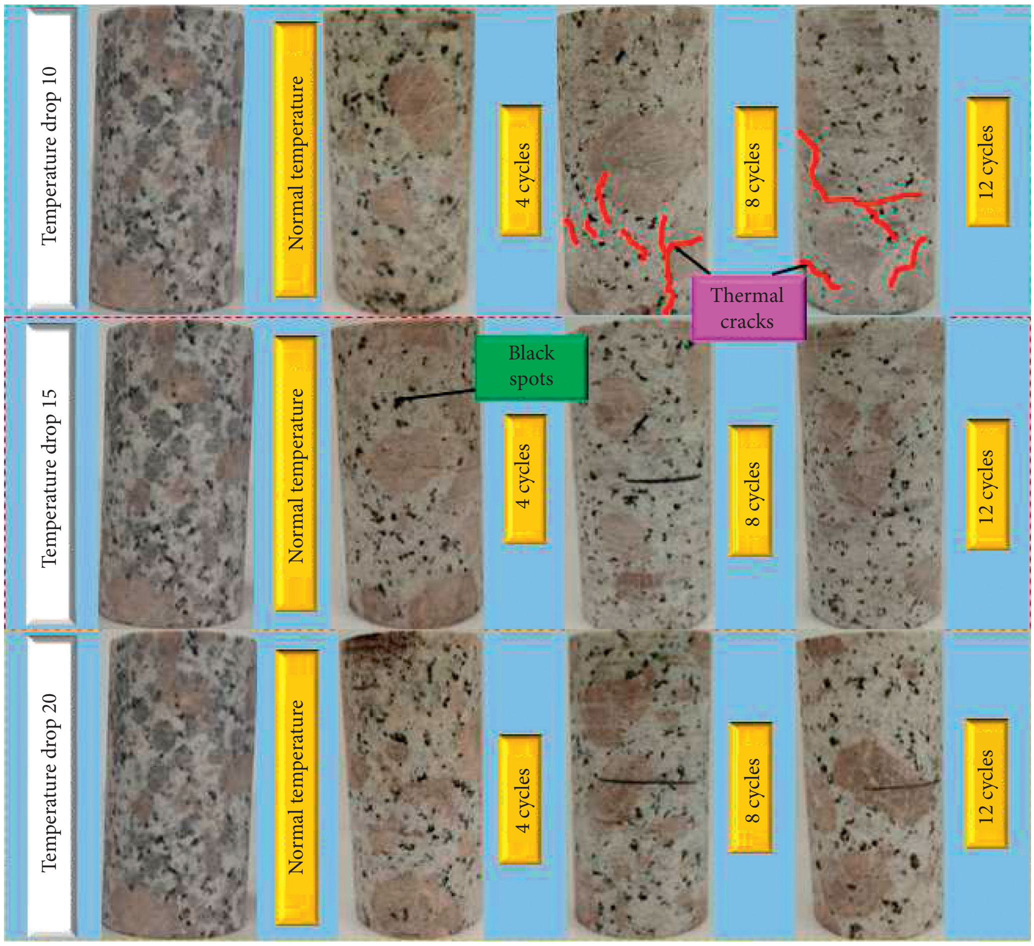

FIGURE 4: Variation characteristics of granite surfaces treated by thermal cycles with uniform-amplitude temperature drops.

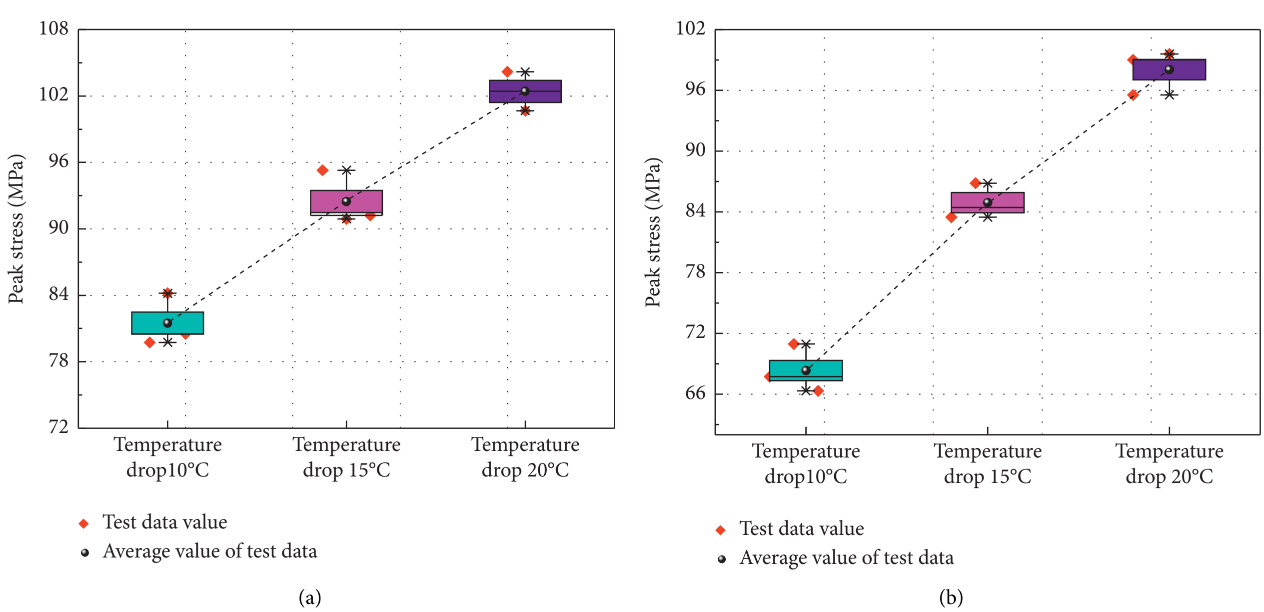

FIGURE 5: Continued.

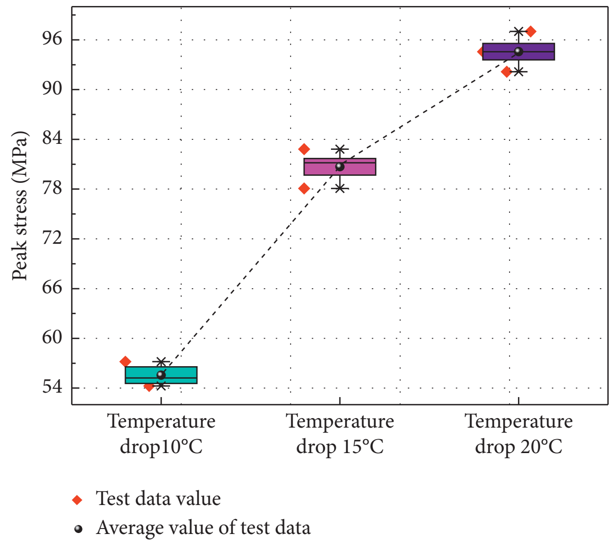

(c)

Figure 5: Variation of the mean peak stress of granite with the temperature drop amplitude. (a) 4 cycles, (b) 8 cycles, (c) 12 cycles.

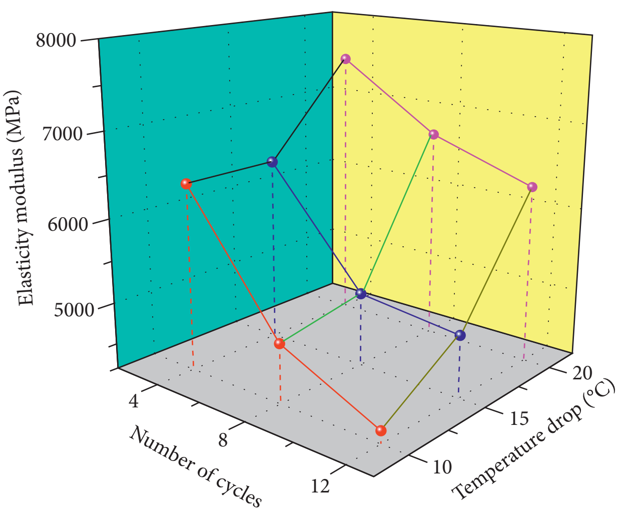

(a)

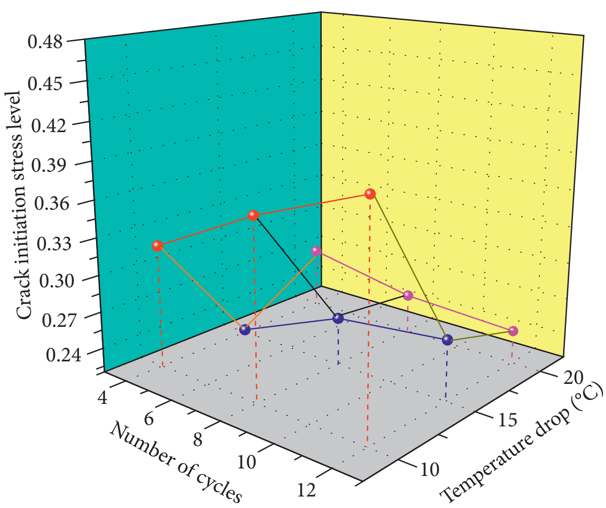

(b)

Figure 6: Elasticity modulus and crack initiation stress level of granite. (a) Elasticity modulus, (b) crack initiation stress level.

increased with the increase of temperature drop amplitude. Also, the crack initiation stress level was lower for a temperature drop amplitude of 20°C compared with that of the 10°C case. The main reason for this phenomenohn was that new microcracks dominated in the granite treated with 15°C and 20°C temperature drops. Otherwise, the thermal stress produced under the condition of temperature drop of 15°C is greater than that of temperature drop of 20°C, so there were more anisotropic microcracks under the 15°C temperature drops compared with the 20°C temperature drops. But when the temperature drop was 10°C, the interconnected microcracks dominated in the granite, leading to reduced microcracks on the whole, which instead improved the heterogeneity of the granite.

3.3. Variation Characteristics of Ringing Count Rate of Granite during Loading. The ringing count rate can directly manifest the damage characteristics of internal rock structures during loading [25]. Figure 7 shows the time evolutions of the ringing count rate, cumulative acoustic emission ringing count rate, and stress. The acoustic emission ringing count rate of granite treated by different temperature drop amplitudes and thermal cycles can be divided into two stages in terms of the loading time: the quiet stage and the active stage. However, affected by the temperature drop amplitudes and thermal cycles, the activity intensity and period of the acoustic emission ringing count rate were varied.

According to Figure 7, the evolution of the acoustic emission ringing count rate basically matched with the

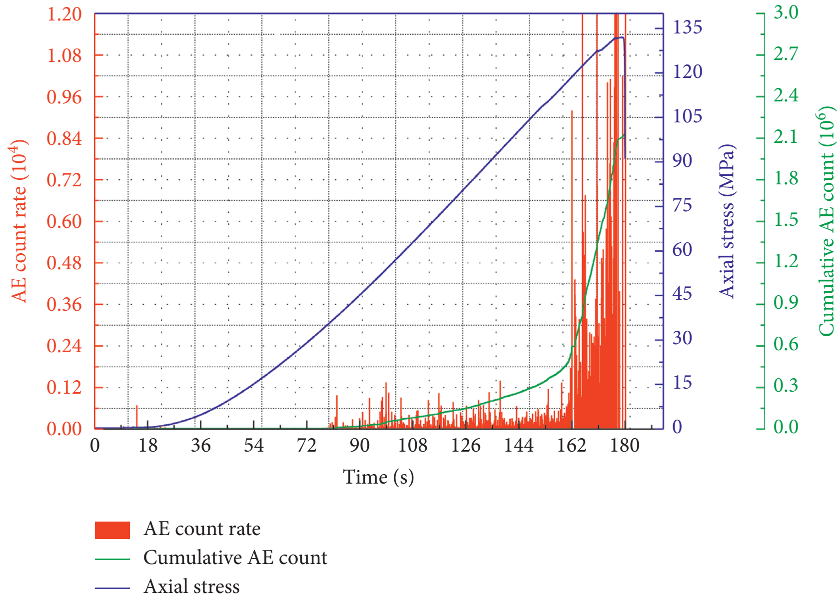

(a)

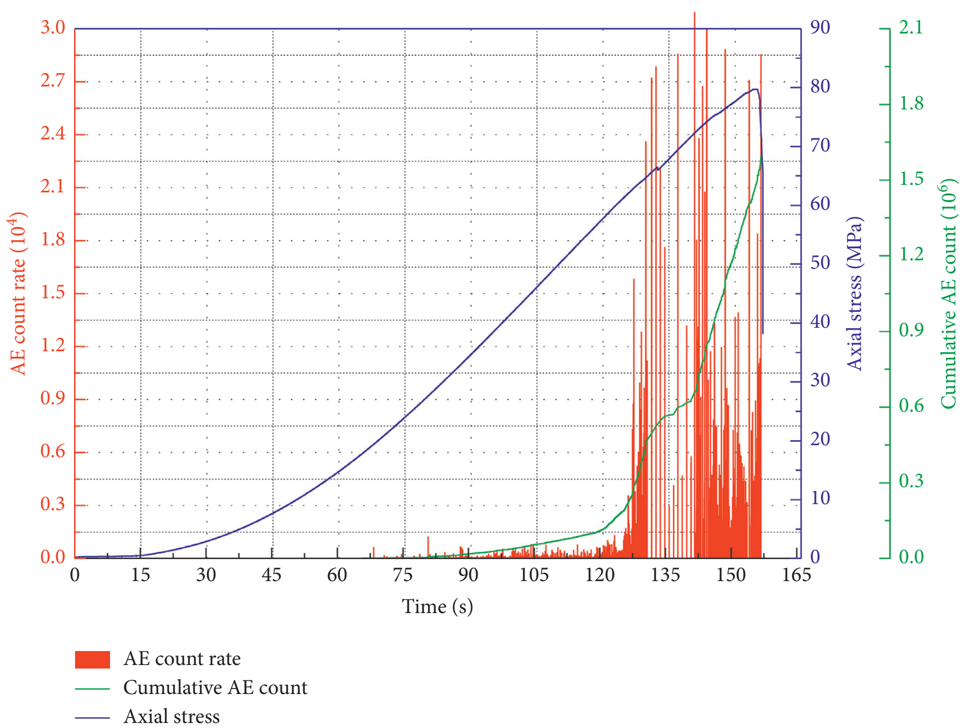

(b)

Figure 7: Continued.

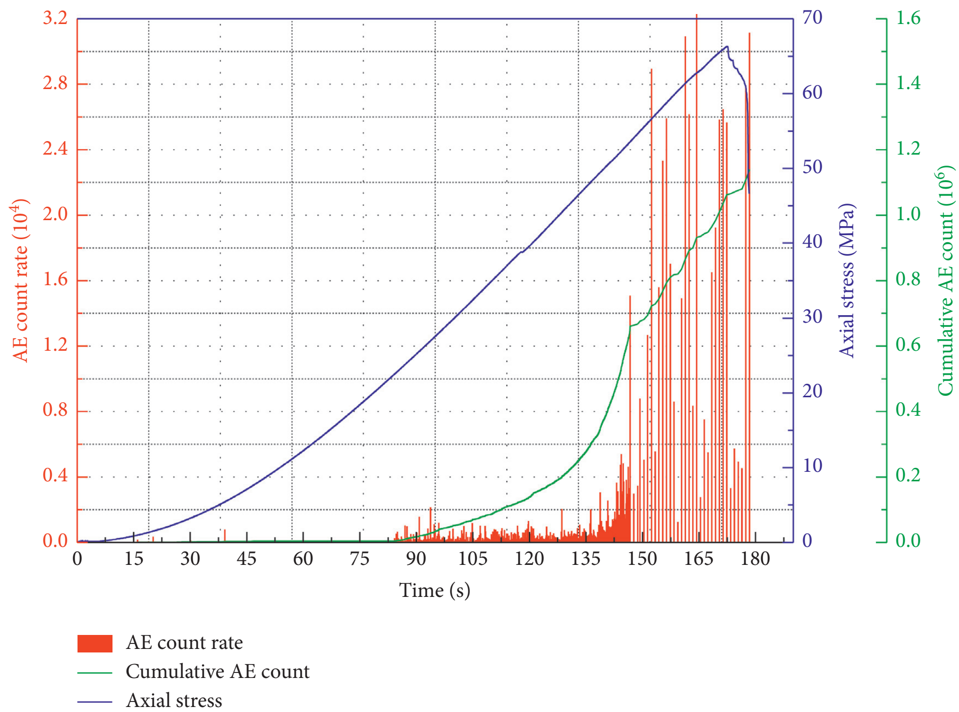

(c)

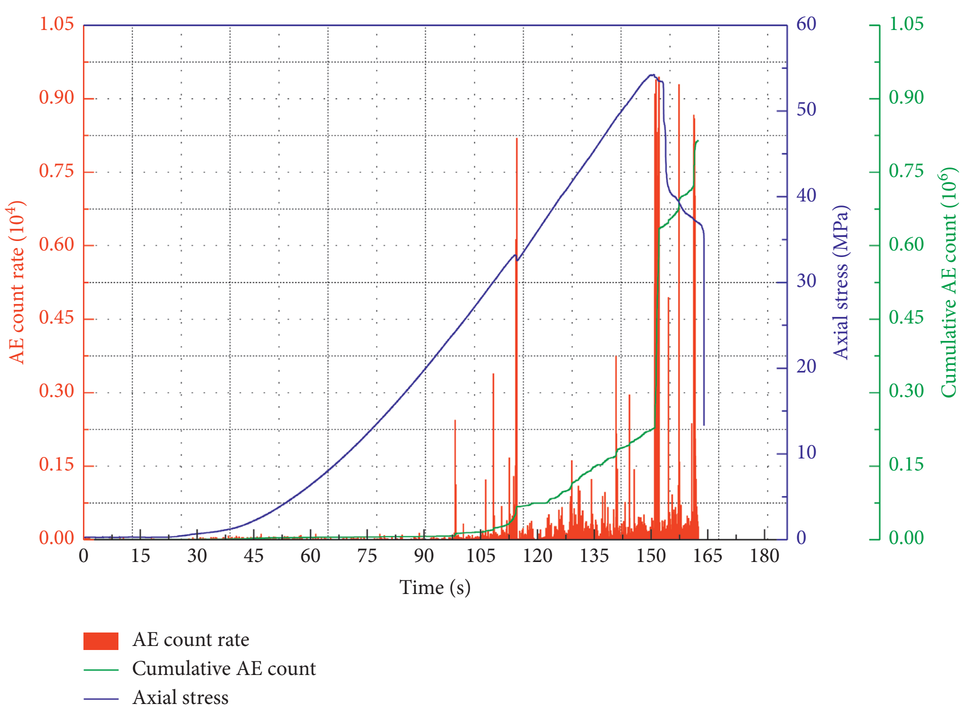

(d)

Figure 7: Continued.

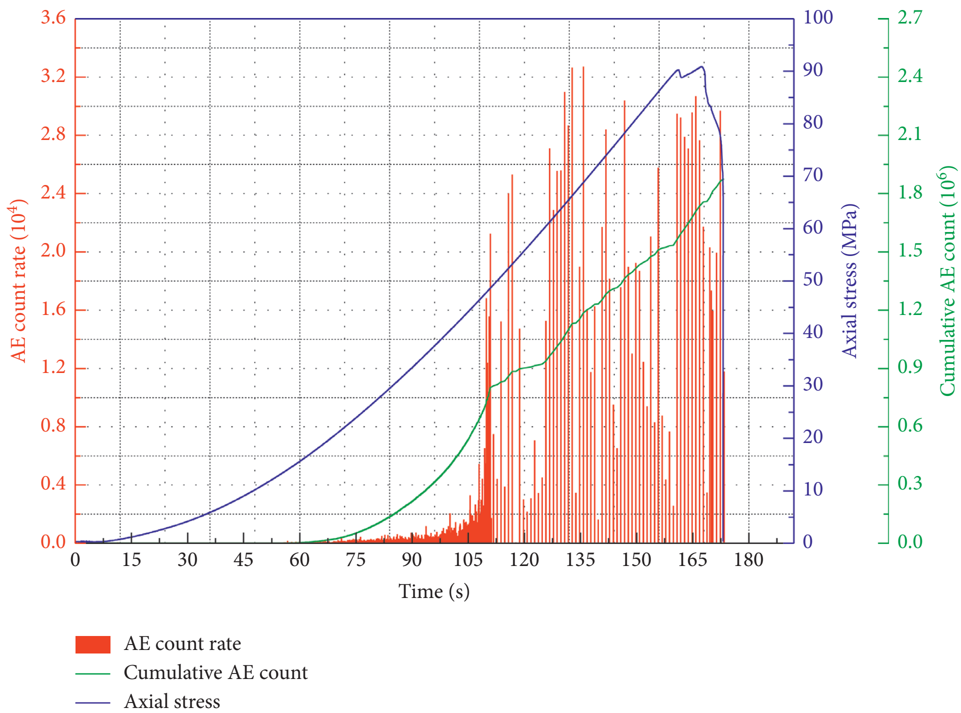

(e)

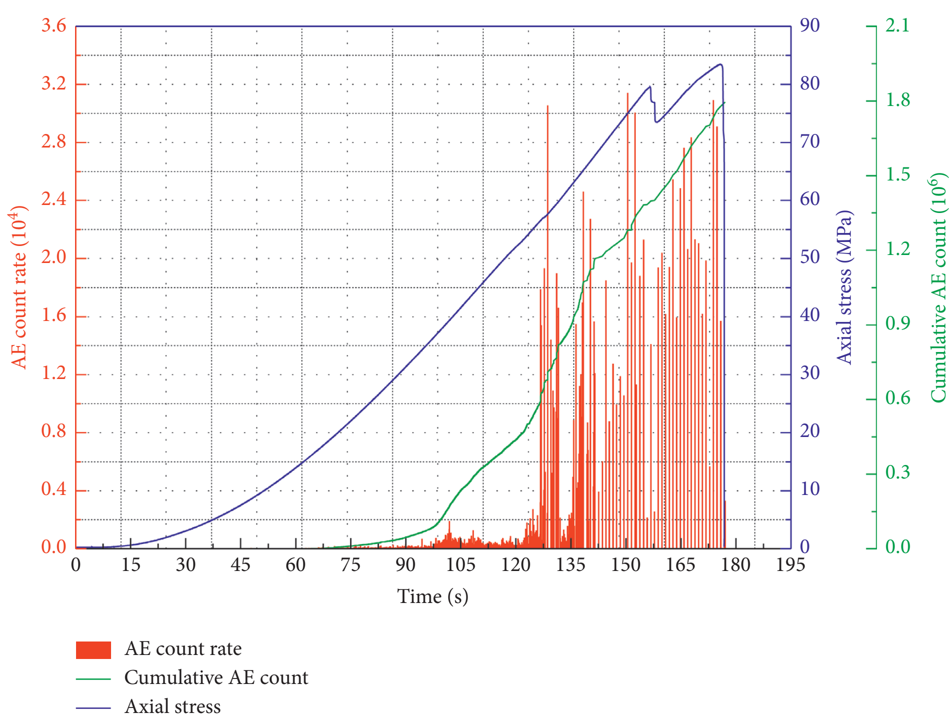

(f)

Figure 7: Continued.

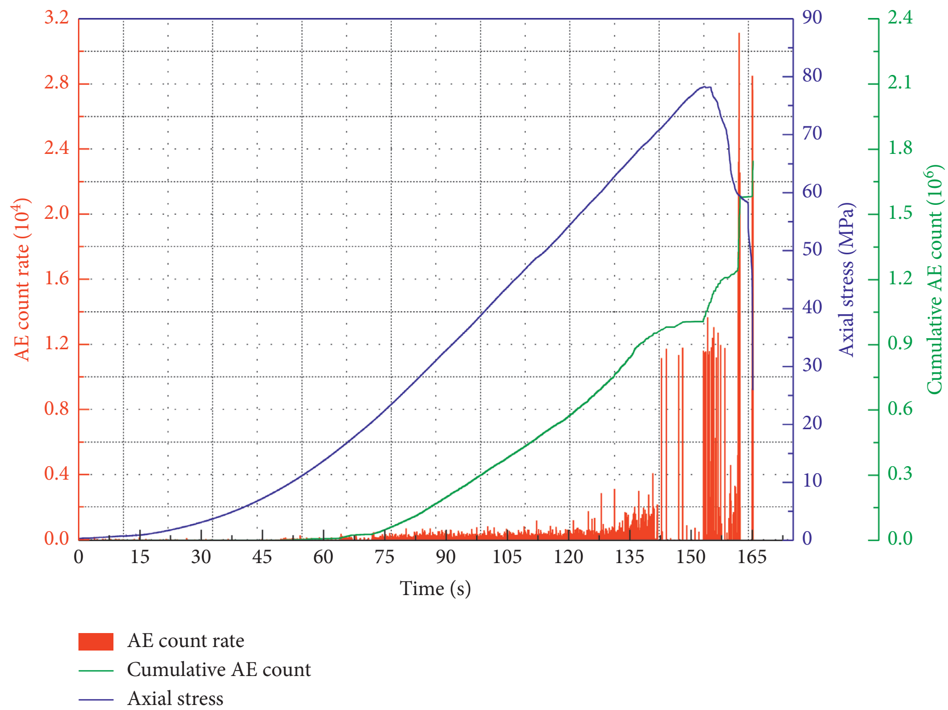

(g)

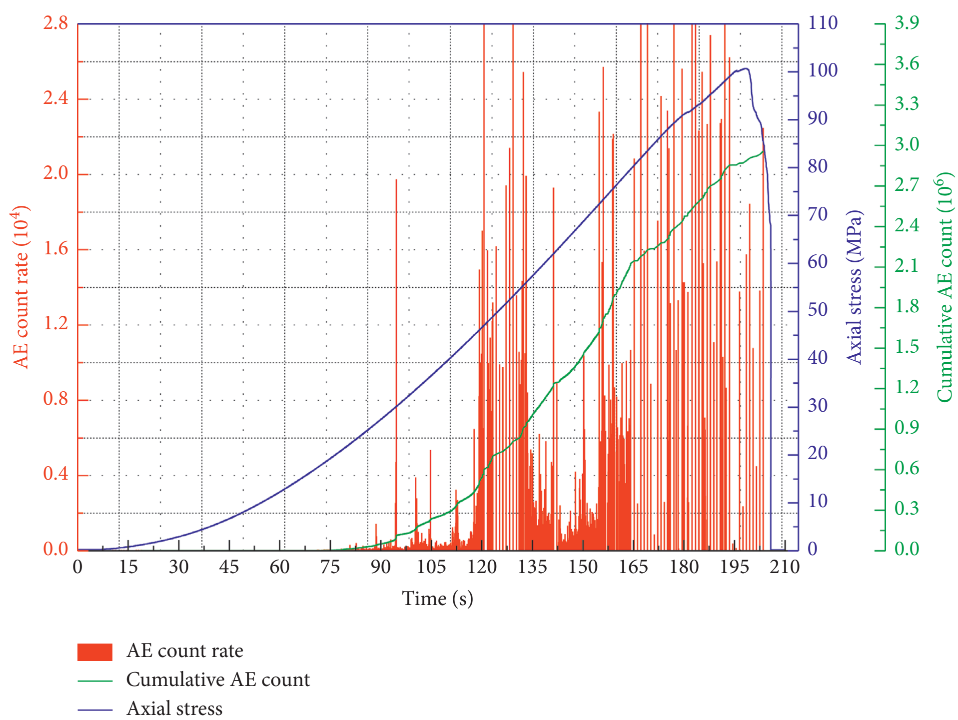

(h)

Figure 7: Continued.

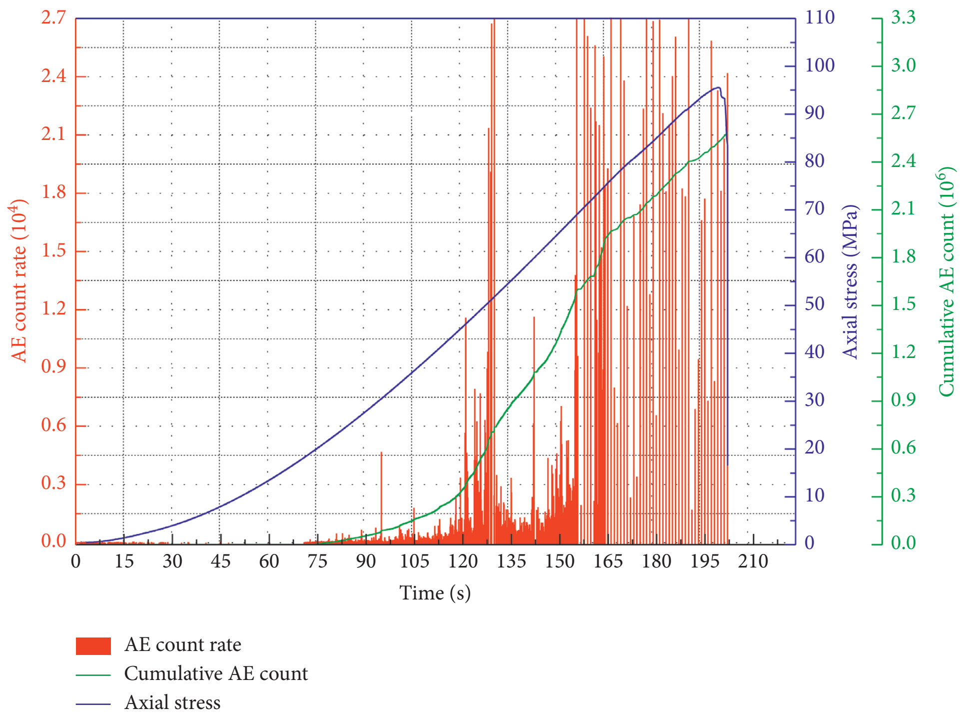

(i)

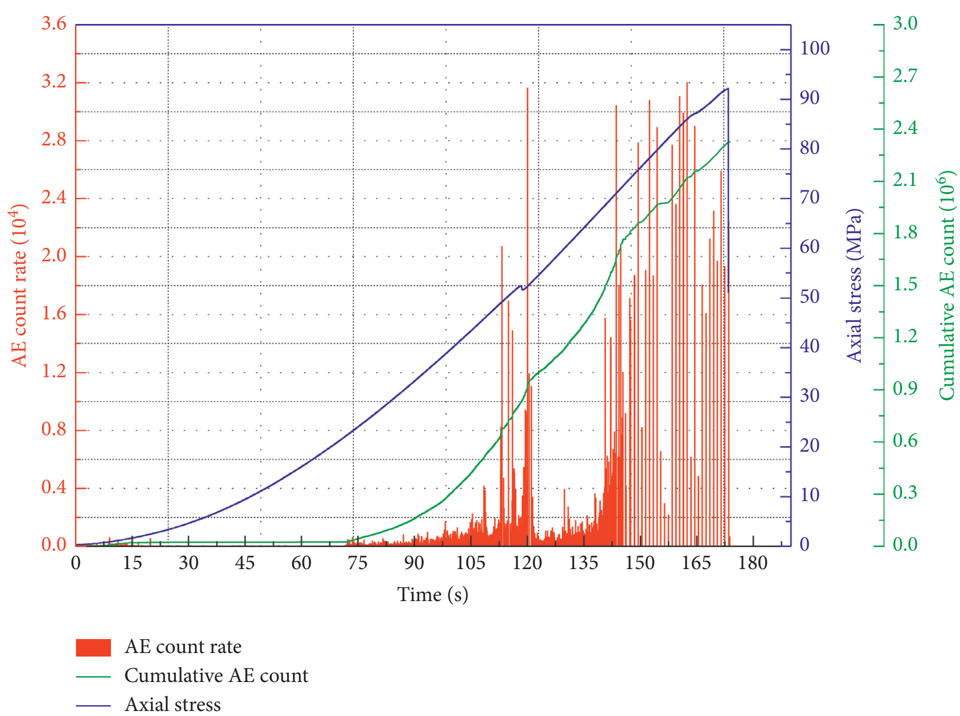

(j)

Figure 7: Time evolutions of stress, acoustic emission ringing count rate, and cumulative ring-down count during loading. (a) Room temperature, (b) temperature drop of 10°C, 4 cycles, (c) temperature drop of 10°C, 8 cycles, (d) temperature drop of 20°C, 12 cycles, (e) temperature drop of 15°C, 4 cycles, (f) temperature drop of 15°C, 8 cycles, (g) temperature drop of 15°C, 12 cycles, (h) temperature drop of 20°C, 4 cycles, (i) temperature drop of 20°C, 8 cycles, (j) temperature drop of 20°C, 12 cycles.

complete stress-time curve. The quiet period of acoustic emission ringing count rate corresponded to the stages of compaction, linear elasticity, and stable expansion of microcracks in the complete stress-time curve. The active period matched the rapid connection of rock cracks and the failure and instability stages in the complete stress-time curve. At room temperature, the internal structure of granite was compact, and the sample was in the quiet period before failure. The acoustic emission ringing count rate remained low in the prepeak loading stage.

Different from the characteristics of acoustic emission ringing count rate at room temperature, when the granite was treated with the 20°C temperature drop for 4 thermal cycles, intense acoustic emission was present on a large scale at the prepeak damage stage. The reason was that the dual effects of high-temperature thermal breaking and water cooling shocks induced plenty of microcracks in the granite structure. Under the influence of axial stress, these microcracks were quickly activated, expanded, and connected, causing strong failure responses in the rock, as a result, a large range of peaks appeared in the prepeak loading stage, and the duration of the quiet period was significantly shortened. However, with the increase of the number of cycles, the duration of the quiet period of acoustic emission ringing count rate began to rise and the cumulative acoustic emission ring-down count decreased. This was primarily due to the fact that the increase of cycles facilitated further development of microcracks, increasing the length and aperture of microcracks, which prolonged the compaction and closing time of microcracks in the loading process.

3.4. Macro and Micro Fracture Characteristics of Granite Treated by Uniform-Amplitude Temperature Drops and Thermal Cycles

3.4.1. Macroscopic Failure Characteristics. The macro failure characteristics can well reflect the damage level of the internal rock structure. The failure modes of the granite under uniaxial compression showed the following rules after treatment with different temperature drop values and thermal cycles (see Figure 8).

(1) At room temperature, the granite structure was dense and its failure mostly belonged to tensile failure [22, 26–28].

(2) After the 20°C temperature drop treatment, microcracks were generated in the granite. Under the influence of axial stress, the microcracks were interconnected to form multiple weak plane structures, the development of which was further promoted by the increasing axial stress. The weak planes approximately parallel to the loading direction were the first to break through their own own tensile strength to form tensile cracks. The weak plane structures with a certain angle in regard to the loading direction also exceeded its own shear strength to form shear cracks. Ultimately, the hybrid tension-shear failure was formed, together with a small amount of fragmented grains. With the increase of the number of thermal cycles, the density of microcracks increased, the area with weak plane structure formations widened, and the number of macro cracks at failure started to increase, though the failure mode was still a hybrid tension-shear one.

(3) When the temperature was dropped by 15°C at each cycle, with the increase of the number of thermal cycles, the granite experienced the transition from the hybrid tension-shear failure mode to the tension failure mode. Specifically, the number of cracks increased significantly, and the failure forms became more fragmented. The main reason for this phenomenon was that the increase of cycles times under this temperature drop amplitude had promoted the formation of weak plane structures before axial loading. When the granite was subjected to axial loading afterwards, the weak plane structures nearly parallel to the loading direction developed preferentially, which in turn inhibited the development of other weak plane structures and eventually induced tensile failure.

(4) At a temperature drop of 10°C, tensile failure dominated in the granite. Also, with the increase of cycle times, local spalling failure appeared. This showed that the granite formed not only a large number of weak plane structures but also locally deteriorated damage areas. Under axial loading, these deteriorated areas were activated to form local spalling areas.

3.4.2. Failure Characteristics of Microstructure. In order to obtain failure characteristics of granite microstructure at different temperature drop values and thermal cycles, the granite slices under different test conditions were observed with a scanning electron microscope, and the AVIZO post-processing software was used to reduce noise, segment, and filter the microstructure images. As shown in Figure 9, the room temperature granite slice was the only sample without microcracks. Apart from that, the other granite slices that experienced different thermal treatments all showed failure and damage in the structure, though with varied degrees. In order to quantitatively compare and analyze the damage of granite structure caused by temperature drops and thermal cycles, the average aperture and average shape factor of microcracks were selected as the indexes to evaluate the damage of granite microstructure.

(1) Microcrack Aperture. With the help of the characteristic that there is a significant gray difference between the image of cracks matrix and rock, we have carried out noise reduction and segmentation of SEM image, and through the MP-Otsu embedded algorithm of AVIZO software, we have obtained the micro-fracture opening of granite under different experimental conditions. Figure 10(a) shows the variation of the average microcrack aperture with the temperature drop amplitude and the number of thermal cycles. It can be seen from Figure 10(a) that under the same number of thermal cycles, the average microcrack aperture increased with the decrease of temperature drop amplitude, this shows that the smaller temperature drop amplitude can promote the increase of microcrack aperture. When the temperature drop gradient was fixed, the average microcrack aperture increased with the increase of the number of thermal cycles. It indicated that the reduction in

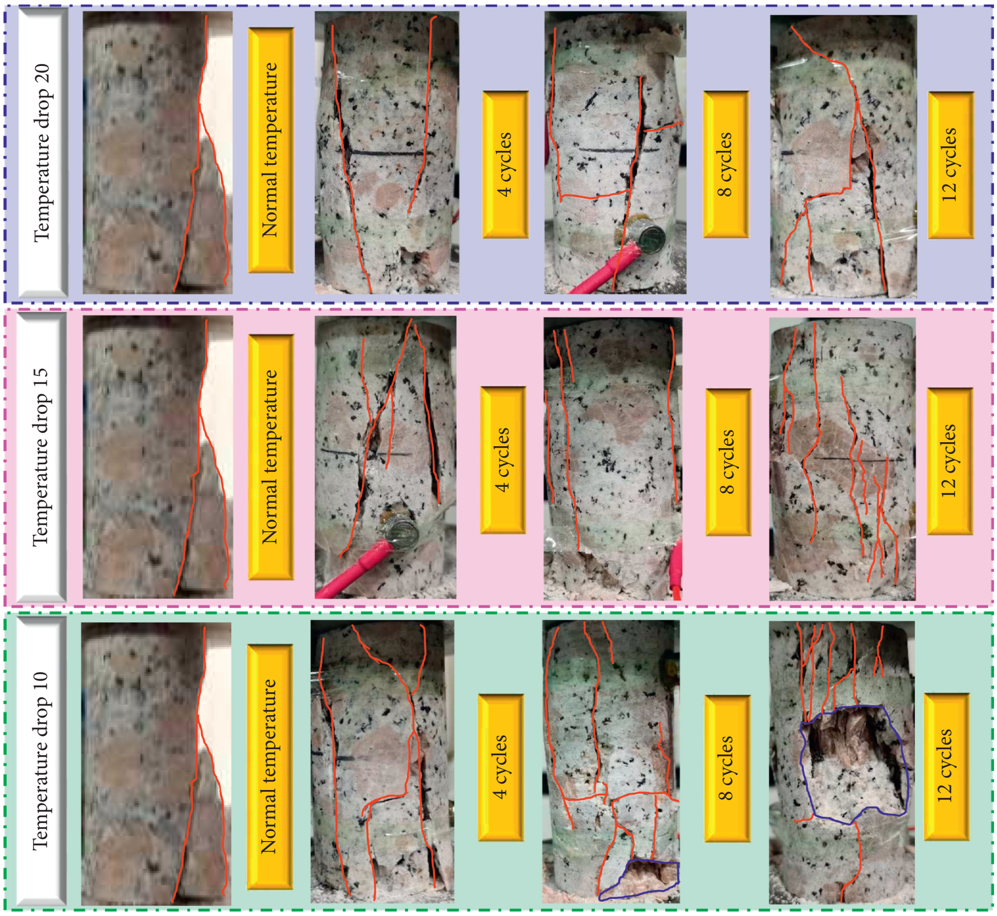

FIGURE 8: Macroscopic failure characteristics of granite treated by thermal cycles with different temperature drop amplitudes.

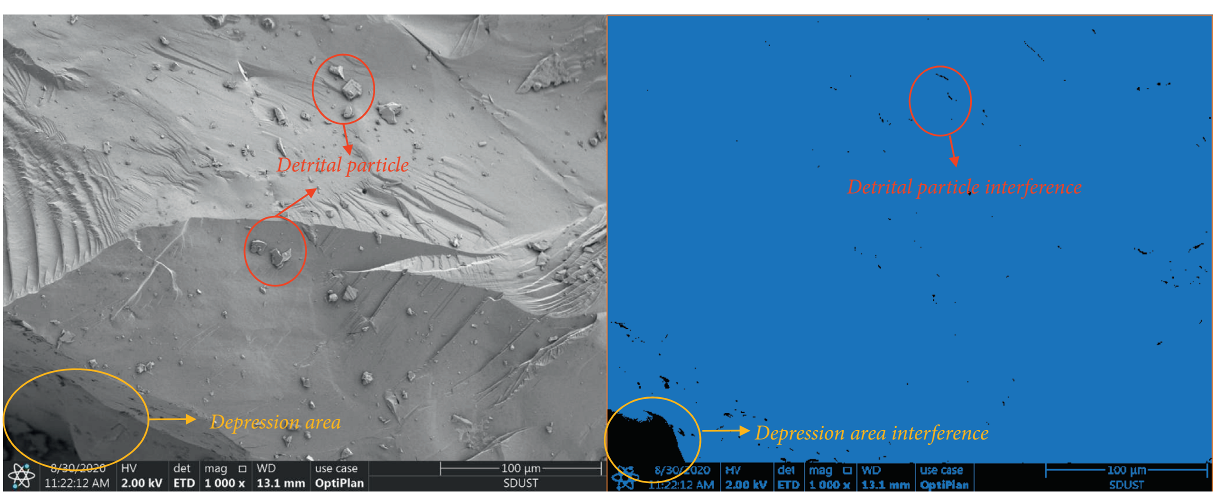

(a)

FIGURE 9: Continued.

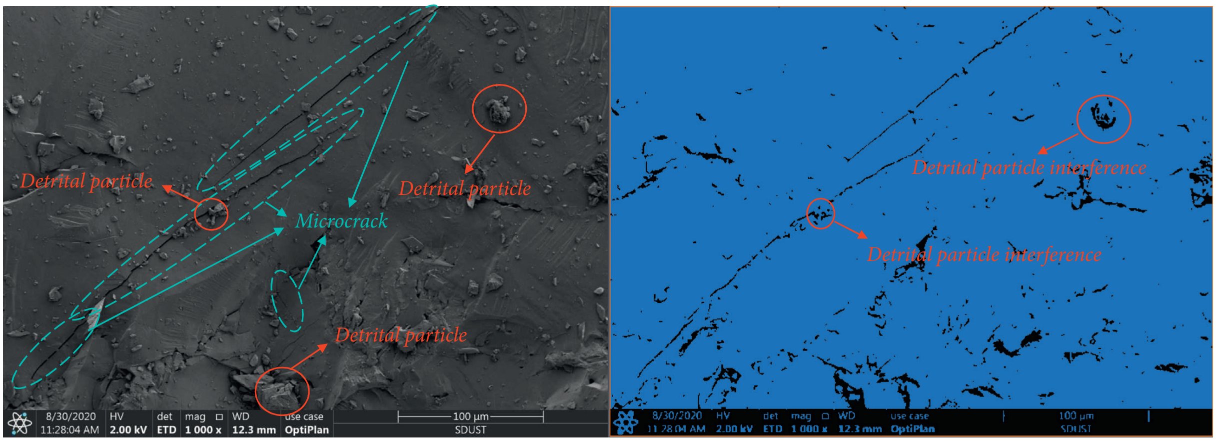

(b)

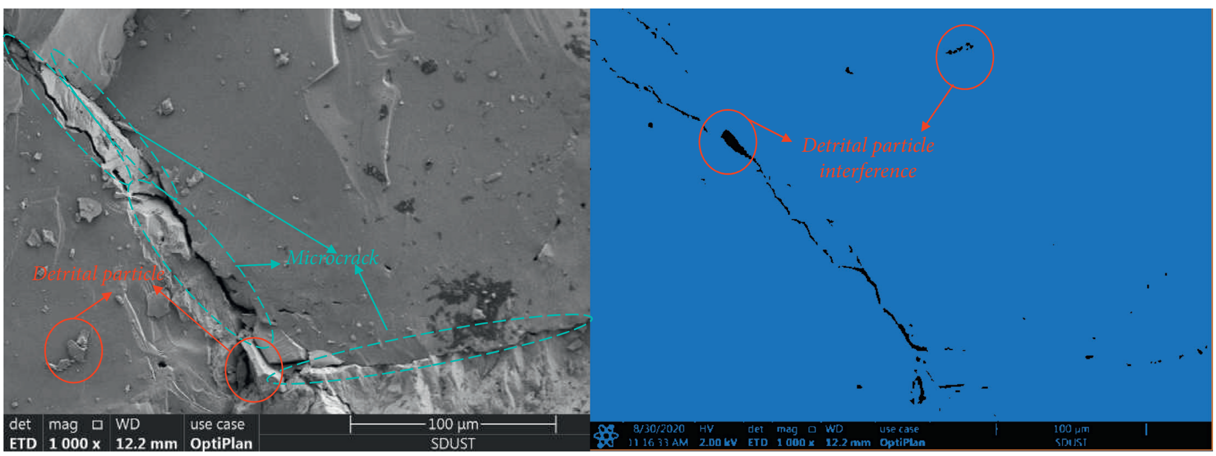

(c)

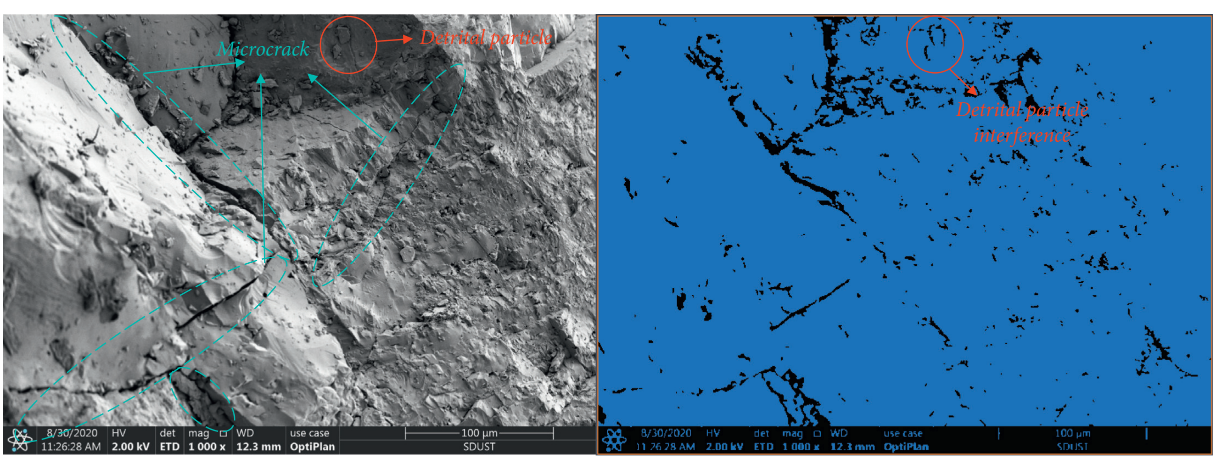

(d)

Figure 9: Continued.

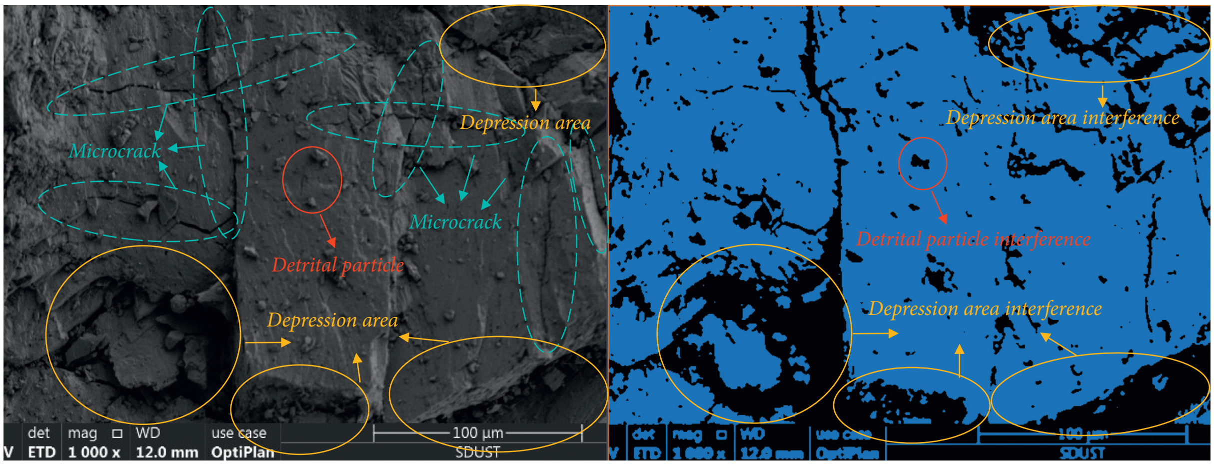

(e)

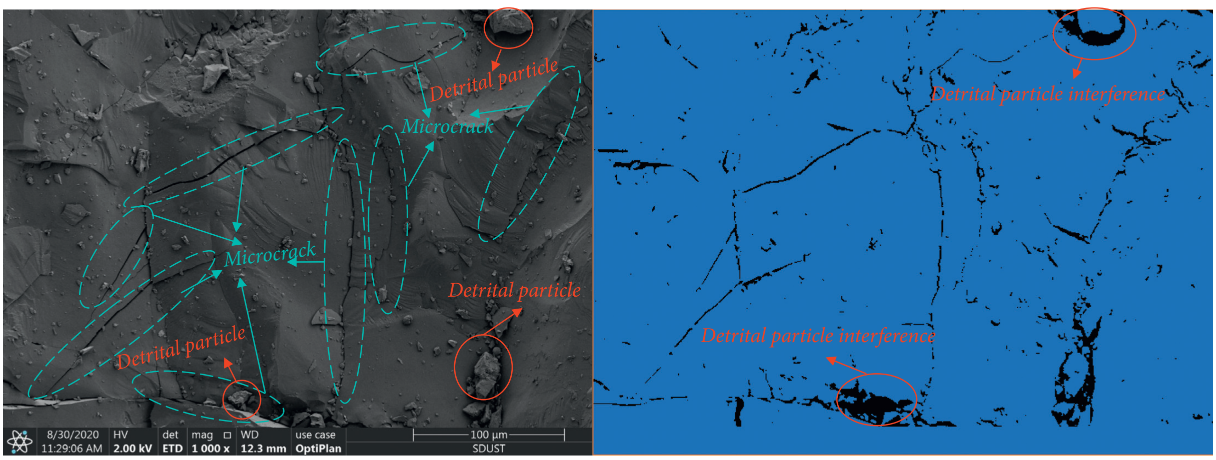

(f)

Figure 9: Micro failure characteristics of granite treated by different temperature drops and thermal cycles. (a) Room temperature, (b) temperature drop of 10°C, 4 cycles, (c) temperature drop of 10°C, 8 cycles, (d) temperature drop of 10°C, 12 cycles, (e) temperature drop of 15°C, 12 cycles, (f) temperature drop of 20°C, 12 cycles.

temperature drop amplitude and the increase in thermal cycles could promote the growth of microcracks, improve the connectivity of microcracks, and thus aggravate the damage of rock structure.

The shape factor of microcracks can be used to characterize the fracture toughness of the microcrack structure itself [29], which can be expressed as

$$Y = \frac{K_I}{\sigma_0 \sqrt{2\pi a}}, \tag{2}$$

where K_1 is the stress intensity factor, σ_0 is the nominal stress when there are no cracks, and a is the radius of the microcrack.

(2) Microcrack Shape Factor. According to equation (2), there exists a positive correlation between the shape factor and the stress intensity factor of the microcrack. The larger the microcrack shape factor is, the greater the stress intensity factor of the microcrack structure is, the easier it is for the microcrack tip to crack and expand, making the rock structure prone to lose its stability. As shown in Figure 10(b), the average microcrack shape factor of granite demonstrated a decreasing trend with the decrease of temperature drop amplitude or the increase of thermal cycles. Referring to the peak stress of granite in Figure 5 and the macro failure characteristics of granite in Figure 9, it could be known that the increase in microcrack shape factor was a main cause for the decrease of peak stress and increase of cracks when the granite was damaged.

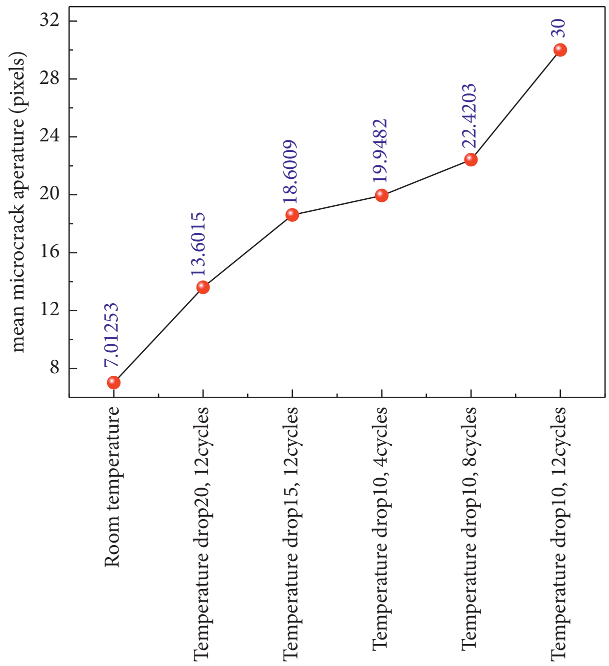

(a)

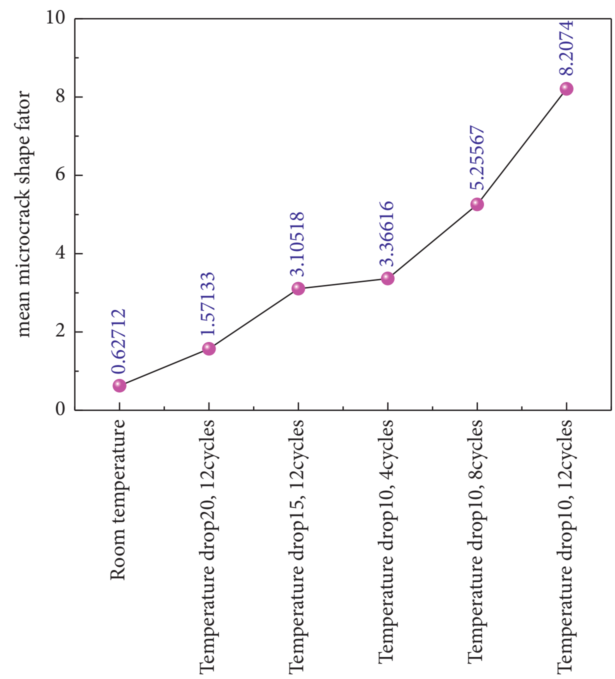

(b)

Figure 10: Mean microcrack aperture and mean microcrack shape factor of granite. (a) Mean microcrack aperture, (b) mean microcrack shape factor.

4. Conclusions

(1) The results have shown that the peak stress and elasticity modulus of granite decreased gradually with the increase of the number of cycles, satisfying the following relationship: 20°C gradient case >15°C gradient case >10°C gradient case. After 8 thermal cycles, the target heating temperature became lower than the threshold temperature of microcracks initiation when the temperature drop amplitudes was 15°C or 20°C, so the peak stress and elasticity modulus tended to be stable under both conditions.

(2) The heterogeneity of granite varied differently with the increase of cycle times under different temperature drop amplitudes. At a temperature gradient of 20°C, the heterogeneity first increased and then tended to be stable. When the temperature was dropped by 15°C at each cycle, the heterogeneity first decreased and then became stable. As for the 10°C scenario, the heterogeneity showed an overall decreasing trend. After 4 cycles, the heterogeneity relationship of granite treated with different temperature drop amplitudes met: 15°C > 20°C > 10°C. However, after 8 cycles, the relationship became 20°C > 15°C > 10°C.

(3) The acoustic emission signal analysis further verified the damage of granite caused by temperature drops and thermal cycles. With the decrease of temperature drop step or the increase of cycle times, the connectivity of microcracks in granite enhanced, the aperture and shape factor of microcracks increased, the damage of granite structure intensified, and the duration of the quiet period in acoustic emission ringing count rate prolonged.

(4) The macro failure mode of granite was significantly affected by the temperature drop amplitude and thermal cycle. At a temperature drop of 10°C, tensile failure dominated in the failure of granite. When the temperature was reduced by 15°C at a time, with the increase of cycle times, the failure mode of granite changed from hybrid tension-shear failure to tension failure. As for the 20°C temperature drop scenario, the failure mode of granite was mainly hybrid tension-shear failure.

Data Availability

The data used to support the findings of this study are available from the corresponding author upon request.

Conflicts of Interest

The authors declare that there are no conflicts of interest regarding the publication of this paper.

Acknowledgments

This research was financially supported by Key Research and Development Plan of Shandong Province (2019SDZY02).

References

[1] C. Li, Y. Q. Hu, C. W. Zhang et al., "Brazilian split characteristics and mechanical properties evolution of granite after cyclic cooling at different temperatures," *Chinese Journal of Rock Mechanics and Engineering*, vol. 39, no. 9, pp. 1–11, 2020.

[2] L. Yu, H. W. Peng, G. W. Li, Y. Zhang, Z. Han, and H. Zhu, "Experimental research on granite under high temperature-water cooling cycle," *Rock and Soil Mechanics*, vol. 42, no. 4, pp. 1–11, 2021.

[3] J. Y. Xie, Z. Q. Chen, and J. Y. Wu, "Mechanical properties and acoustic emission response characteristics of granite after cyclic high temperature-rapid cooling treatment," *Journal of Engineering Geology*, vol. 29, pp. 1–9, 2020.

[4] G. Rong, S. Sha, B. Li, Z. Chen, and Z. Zhang, "Experimental investigation on physical and mechanical properties of granite subjected to cyclic heating and liquid nitrogen cooling," *Rock Mechanics and Rock Engineering*, vol. 54, no. 5, pp. 2383–2403, 2021.

[5] J. Peng, G. Rong, Z. Tang, and S. Sha, "Microscopic characterization of microcrack development in marble after cyclic treatment with high temperature," *Bulletin of Engineering Geology and the Environment*, vol. 78, no. 8, pp. 5965–5976, 2019.

[6] P. K. Gautam, R. Dwivedi, A. Kumar et al., "Damage characteristics of jalore granitic rocks after thermal cycling effect for nuclear waste repository," *Rock Mechanics and Rock Engineering*, vol. 54, no. 1, pp. 235–254, 2020.

[7] S. V. Pathiranagei and I. Gratchev, "Engineering properties of sandstone heated to a range of high temperatures," *Bulletin of Engineering Geology and the Environment*, vol. 80, no. 3, pp. 2415–2432, 2021.

[8] L. Yu, H. W. Peng, Y. Zhang, and G.-w. Li, "Mechanical test of granite with multiple water-thermal cycles," *Geothermal Energy*, vol. 9, no. 1, pp. 1–15, 2021.

[9] F. Zhao, Q. Sun, and W. Zhang, "Fractal analysis of pore structure of granite after variable thermal cycles," *Environmental Earth Sciences*, vol. 78, no. 24, p. 677, 2019.

[10] Astm, *Standard Test Methods for Compressive Strength and Elastic Moduli of Intact Rock Core Specimens under Varying States of Stress and Temperatures*, ASTM International, West Conshohocken, PA, USA, 2014.

[11] S. Shao, P. G. Ranjith, P. L. P. Wasantha, and B. K. Chen, "Experimental and numerical studies on the mechanical behaviour of Australian Strathbogie granite at high temperatures: an application to geothermal energy," *Geothermics*, vol. 54, pp. 96–108, 2015.

[12] W. G. P. Kumari, P. G. Ranjith, M. S. A. Perera, B. K. Chen, and I. M. Abdulagatov, "Temperature-dependent mechanical behaviour of Australian Strathbogie granite with different cooling treatments," *Engineering Geology*, vol. 229, pp. 31–44, 2017.

[13] Z. C. Tang, M. Sun, and J. Peng, "Influence of high temperature duration on physical, thermal and mechanical properties of a fine-grained marble," *Applied Thermal Engineering*, vol. 156, pp. 34–50, 2019.

[14] Y.-J. Shen, J.-S. Hao, X. Hou, J.-Q. Yuan, and Z.-P. Bai, "Crack propagation in high-temperature granite after cooling shock: experiment and numerical simulation," *Bulletin of Engineering Geology and the Environment*, vol. 80, no. 7, pp. 5831–5844, 2021.

[15] Y. J. Shen, J. Q. Yuan, X. Hou, J. Hao, Z. Bai, and T. Li, "The strength changes and failure modes of high-temperature granite subjected to cooling shocks," *Geomechanics and Geophysics for Geo-Energy and Geo-Resources*, vol. 7, 2021.

[16] Y.-j. Shen, X. Hou, J.-q. Yuan, and C.-h. Zhao, "Thermal cracking characteristics of high-temperature granite suffering from different cooling shocks," *International Journal of Fracture*, vol. 225, no. 2, pp. 153–168, 2020.

[17] C. H. Zhang, S. You, and H. G. Ji, "Grain-based model and analysis of deep hard rock considering intragranular structure characteristics of mineral," *Journal of China Coal Society*, pp. 1–11, 2021.

[18] F. Q. Wu, L. Qiao, S. G. Guan, Q. T. Zhang, Z. Y. Wang, and J. Wu, "Study on size effect of uniaxial compression tests of small size rock samples," *Chinese Journal of Rock Mechanics and Engineering*, vol. 15, pp. 1–9, 2021.

[19] D. Y. Fan, X. S. Liu, Y. L. Tan, S.-L. Song, J.-G. Ning, and Q. Ma, "Numerical simulation research on response characteristics of surrounding rock for deep super-large section chamber under dynamic and static combined loading condition," *Journal of Central South University*, vol. 27, no. 12, pp. 3544–3566, 2020.

[20] Q. Ma, Y. L. Tan, X. S. Liu, Q. Gu, and X. Li, "Effect of coal thicknesses on energy evolution characteristics of roof rock-coal-floor rock sandwich composite structure and its damage constitutive model," *Composites Part B*, vol. 198, 2020.

[21] Y. P. Qiu and Z. Y. Lin, *Correlation between Crack Initiation Stress Level and Brittleness Index*, Shanghai Jiaotong University, Shanghai, China, 2014.

[22] X. S. Liu, D. Y. Fan, Y. L. Tan et al., "Failure evolution and instability mechanism of surrounding rock for close-distance parallel chambers with super-large section in deep coal mines," *International Journal of Geomechanics*, vol. 21, no. 5, 2021.

[23] X. S. Liu, S. L. Song, Y. L. Tan et al., "Similar simulation study on the deformation and failure of surrounding rock of a large section chamber group under dynamic loading," *International Journal of Mining Science and Technology*, vol. 31, no. 3, pp. 495–505, 2021.

[24] X. S. Liu, D. Y. Fan, Y. L. Tan et al., "New detecting method on the connecting fractured zone above the coal face and a case study," *Rock Mechanics and Rock Engineering*, vol. 54, 2021.

[25] L. T. Dou, K. Yang, and X. L. Chi, "Fracture behavior and acoustic emission characteristics of sandstone samples with inclined precracks," *International Journal of Coal Science and Technology*, vol. 8, no. 1, pp. 77–87, 2021.

[26] Y. Wu, X. Z. Li, Z. Huang, W. T. Xu, L. C. Deng, and M. Z. Liu, "Deformation and failure characteristics of granite under uniaxial compression after high temperature," *Journal of Engineering Geology*, vol. 28, no. 2, pp. 240–245, 2020.

[27] S. L. Song, X. S. Liu, Y. L. Tan, D. Fan, Q. Ma, and H. Wang, "Study on failure modes and energy evolution of coal-rock combination under cyclic loading," *Shock and Vibration*, vol. 2020, Article ID 5731721, 16 pages, 2020.

[28] J. P. Zuo, J. T. Wang, and Y. Q. Jiang, "Macro/meso failure behavior of surrounding rock in deep roadway and its control technology," *International Journal of Coal Science and Technology*, vol. 6, no. 3, pp. 301–319, 2019.

[29] T. Wang, J. G. Yang, X. S. Liu, Z. B. Dong, and H. Y. Fang, "Influence of joint geometric parameters on shape factor of under-matched butt joint with center crack," *Transactions of the China Welding Institute*, vol. 33, no. 1, pp. 101–104, 2012.